

Pressure stability and low compressibility of intercalated cagelike materials: The case of silicon clathrates

A. San-Miguel,¹ P. Mélinon,¹ D. Connétable,¹ X. Blase,¹ F. Tournus,¹ E. Reny,² S. Yamanaka,² and J. P. Itié³

¹*Département de Physique des Matériaux, Université Claude Bernard-Lyon 1 and CNRS, 43 Bld., 11 Novembre 1918, 69622 Villeurbanne, France*

²*Department of Applied Chemistry, Faculty of Engineering, Hiroshima University, Higashi-Hiroshima 739-8527, Japan and CREST, Japan Science and Technology Corporation (JST), Kawaguchi 332-0012, Japan*

³*L.U.R.E., Centre Universitaire Paris-Sud, Bat., 209D, BP34, 91898 Orsay, France*

(Received 21 September 2001; published 11 January 2002)

We study the behavior under pressure (up to 35 GPa) of intercalated silicon clathrates, combining x-ray diffraction experiments and *ab initio* calculations. We show that endohedral doping does not introduce a strong modification of the compressibility of the empty clathrate network and that in particular cases can raise it to values equivalent to the one of the silicon diamond phase. Intercalation can also prevent the collapse of the cage structure up to pressures at least 3 times higher than in the empty clathrate. Further we find that the stability of all studied silicon clathrate networks as well as stressed silicon diamond is limited to average Si-Si interatomic distances higher than 2.30 Å.

DOI: 10.1103/PhysRevB.65.054109

PACS number(s): 61.50.Ks, 61.50.Lt, 64.70.Kb, 71.15.Nc

Silicon clathrates are cubic three dimensional (3D) arrangements of sp^3 -based distorted tetrahedral units of Si_{20} and Si_{24} cages (type I, labeled Si-46 or Si_{46} , space group $Fd\bar{3}m$) or Si_{20} and Si_{28} cages (type II, labeled Si-34 or Si_{136} , space group $\pm\bar{3}n$) (Fig. 1). These cubic structures are isomorphous with ice or SiO_2 clathrates (clathrasils) and are characterized by a large predominance of pentagonal rings (up to 86% in type II). Even though such low-density phases of Si were first synthesized about 35 years ago,¹ it is only recently that several experimental and theoretical studies have shown that such materials display remarkable properties in the fields of superconductivity,² thermoelectric applications,³ magnetism⁴ or wide-band-gap semiconductors.^{5,6} In a recent study of the high-pressure structural properties of Si-34 clathrates,⁷ it was also shown that its bulk modulus B_0 is $\sim 10\%$ smaller than the one of the diamond Si-2 phase and that it undergoes a phase transformation towards the β -tin phase at the same pressure (11.5 GPa) as does diamond silicon, a surprising result for such a low-density structure.

The cagelike topology of clathrate phases allows further the introduction of guest atoms (M) in the cages ($M_x@Si-46$, for instance, with all cages full when $x=8$).⁸ Intercalation is well known to modify the electronic properties of the host network (as in the case of graphite or C_{60} phases) as well as structural properties under pressure.^{14,9} In particular, in the case of the Si-46 clathrate, the system becomes metallic under intercalation by Na (Ref. 10) or Ba (Refs. 2 and 11).

Here we study the pressure stability and compressibility of endohedrally doped silicon clathrates $M_8@Si-46$ with $M=Na, Ba, \text{ and } I$. Combining experimental results and *ab initio* calculations, we find that endohedral doping of silicon clathrates does not alter the compressibility of the empty clathrate or can even decrease it to values attaining the one of the diamond Si-2 phase. Further, we show that selective intercalation can prevent the collapse of the clathrate structure up to very high pressures. Finally we show that the

stability of the silicon network is associated with a limiting value of the bond distance between the silicon atoms.

There has been considerable interest in the high-pressure properties of ice-based clathrates.¹²⁻¹⁴ Even if the ice clathrates become unstable at moderated pressures, methane hydrate clathrate maintains hydrated character at least up to 9 GPa.¹⁴ A limited number of investigations have been performed on the high-pressure properties of silica clathrates (clathrasils) for which reversibly high-pressure amorphization has been found when intercalated.¹⁵

We have studied the high-pressure properties of $Na_{16}Ba_{17}$ and the recently synthesized iodine-doped $Si-46$ clathrate¹⁸ by x-ray powder diffraction in the energy dispersive DW11 station of the LURE synchrotron (Orsay, France). We note that in the case of the iodine clathrate, the proposed stoichiometry is $I_8Si_{46-x}I_x$ ($x=1.5\pm 0.5$), but we will use the more simple $I_8@Si-46$ notation and discuss the effect of stoichiometry when necessary. The experimental protocol is analogous to the one described in Ref. 7. Diamond anvil cells (DAC's) were loaded with an homogeneous mixture of fine-grained sample powder and silicon oil. The preparation of an homogeneous suspension of the sample powder in silicon oil allowed us to reduce grain-bridging nonhydrostatic effects that we have easily encountered when using other pressure transmitting media. Tiny ruby chips of less than 5 μm of diameter were used for the pressure calibration. The uncertainty of the pressure measurement is of $\pm 5\%$. In one of the experiments on $Ba_8@Si-46$, the ruby signal was lost between 9.3 and 15.6 GPa and we used the membrane pressure of our membrane-type DAC for the pressure calibration. For this particular set of points the uncertainty was estimated to be $\pm 10\%$. Our diffraction data do not allow us to check for an evolution of the atomic positions inside the unit cell due to preferred orientation effects. Nevertheless, we have verified through *ab initio* calculations (see below) that the values of the coordinates defining the positions of the silicon atoms in the type-I clathrate structure are nearly independent of pressure.¹⁹

We show in Fig. 2 some selected diffraction patterns of

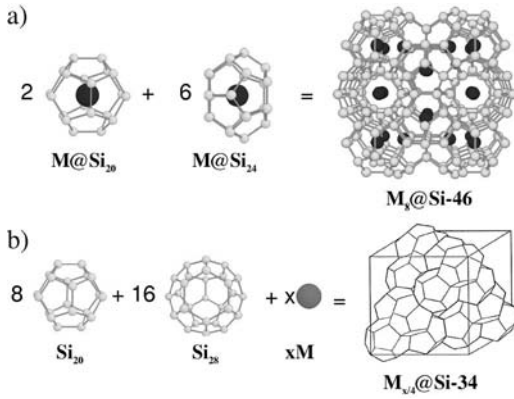


FIG. 1. The structure of silicon clathrates of type I (a) and II (b) can be viewed as cubic 3D arrangements of face-sharing fullerene-like units. The clathrate topology allows the introduction of guest atoms (M) in the cages. The case $M_8\text{@Si-46}$ corresponds to the type-I clathrate with all cages full with one guest atom

$\text{Ba}_8\text{@Si-46}$ and $\text{I}_8\text{@Si-46}$ at different pressures. In both cases the peaks of the cubic clathrate structure can be followed up to the highest measured pressure (35 GPa). In the case of $\text{Ba}_8\text{@Si-46}$ and for pressures above 30 GPa, only the most intense peaks are observed. At higher pressures we observe a diminution of the diffraction peak intensity and at 35 GPa only wide peaks corresponding to the most intense (210) and (211) reflections could be observed (Fig. 2). Signs of amorphization in the background signal were difficult to detect due to the strong Compton scattering from the diamond anvils. The evolution of the cell parameter for $\text{Ba}_8\text{@Si-46}$ and $\text{I}_8\text{@Si-46}$ is shown in Fig. 3(a). We observe a change in the pressure dependence of the cell parameter at about 13 GPa for the Ba clathrate and at 17 GPa for the

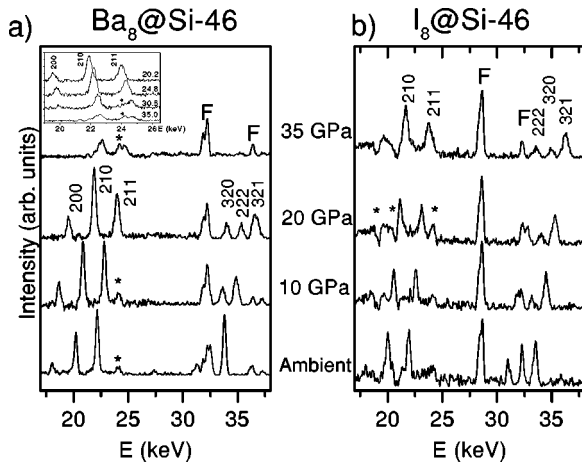


FIG. 2. Background-subtracted energy-dispersive x-ray diffraction patterns as a function of pressure of intercalated clathrates: (a) $\text{Ba}_8\text{@Si-46}$ and (b) $\text{I}_8\text{@Si-46}$. Pressure is indicated in between both panels. The indexation is for the clathrate structure while F holds for x-ray fluorescence. The stars indicate background glitches at fixed energies. Differences in the background noise are due to the optimization of the counting time. The inset in (a) shows details of the x-ray patterns in the high-pressure region.

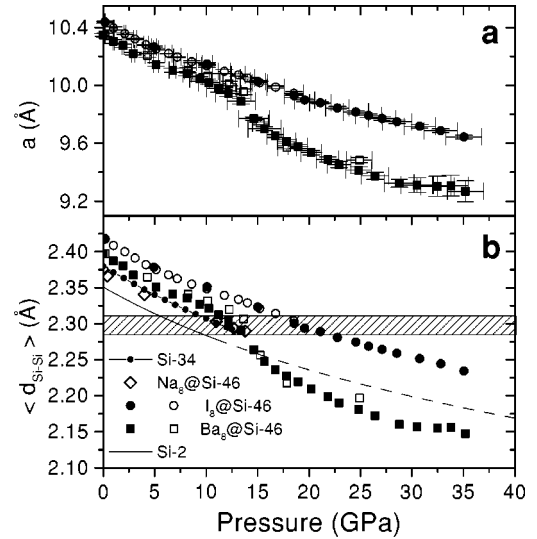


FIG. 3. Pressure dependence of characteristic structural parameters of barium and iodine clathrates: (a) cell parameter and (b) average first-neighbor Si-Si distance. The hatched region corresponds to the stability limit of the clathrate structure. The values of the mean distance above the stability limit are calculated assuming an isostructural transition without modification of the ambient internal crystallographic coordinates. Open and solid symbols correspond to two separate experiments.

iodine one. This was confirmed in two separate experiments for the Ba clathrate. In the case of $\text{Na}_8\text{@Si-46}$, few diffraction patterns could be acquired, but the normal compression of the clathrate structure was followed by the crystallization of the silicon hexagonal high-pressure structure above 14 GPa. Before discussing the details of the evolution of doped clathrates after the phase transition, we will first consider the effect of intercalation on the compressibility and second the stability of the clathrate structure.

The experimental (P, V) data points can be well fitted with the Murnaghan equation of state giving bulk modulus values that are summarized in Table I. In $\text{Na}_8\text{@Si-46}$ the acquired data were insufficient for this analysis and are not included. Within our error bars, our data do not allow a clear-cut conclusion and we have performed *ab initio* calculations to better understand the effect of intercalation on clathrate compressibility.

Our *ab initio* calculations were done within the local density approximation to the density functional theory.²⁰ We adopt a pseudopotential approach²¹ and a plane-wave expansion of the wave functions. We focus in particular on $\text{I}_8\text{@Si-46}$ for which no theoretical study exists. After structural relaxation, we find that iodine atoms are stabilized by 0.64 eV when located inside the Si cages as compared to their energy in I_2 dimers. This surprisingly large binding energy for iodine inside the Si cages indicates a strong I-Si interaction.

A Murnaghan fit of the energy versus volume data points for the iodine clathrate yields $B_0 = 91$ GPa, which is 4% larger than the one of the undoped Si-46 clathrate, despite the 2.4% volume increase of the unit cell volume under iodine intercalation. The large I binding energy and the in-

TABLE I. Bulk modulus B_0 of silicon clathrates compared to the one of the diamond structure.

Compound	Experimental	Calculations	
	B_0 (GPa)	B_0 (GPa)	Difference from Si-2 (%)
Xe ₈ @Si-46	Not synthesized	85 ^a	12
Si-46	Not synthesized	87 ^a	10
Si-34	90 ± 5 ^b	87.5 ^b	9.5
Ba ₈ @Si-46	93 ± 5 ^a	-	-
I ₈ @Si-46	95 ± 5 ^a	91 ^a	6
Te ₈ @Si-46	Not synthesized	95 ^a	2
Sn ₈ @Si-46	Not synthesized	97 ^a	0
Si-2 (diamond)	97.88 ^c	97 ^b	0

^aThis work.

^bReference 7.

^cReference 24.

crease of B_0 point again to a mixing of the iodine and silicon orbitals to form ionocovalent bonds.²²

Possible factors intervening in the lower compressibility of the iodine clathrate as compared to the empty one (Si-46) are the guest-host interaction and/or the lattice dilatation due to the “volume-excluded” (or steric) effect. To try to quantify the steric effect we have calculated the compressibility of hypothetical Xe₈@Si-46 for which the atomic size is similar and the guest-host interaction will be very low, as the rare-gas atom Xe is expected to be chemically inert. We have found a bulk modulus value of 85 GPa, which is, respectively, 3% and 6% smaller than in Si-46 and I₈@Si-46. This demonstrates that the lower compressibility of I₈@Si-46 is not related to a steric effect but to electronic mixing.

In our case, the chemical host-guest coupling can be decomposed in a covalent and a ionic part due to the guest-host electronegativity difference. To test the effect of covalency, we consider the hypothetical Sn₈@Si-46 for which we obtain a bulk modulus value of 97 GPa, which is the same as in silicon diamond and larger than for the iodine clathrate. This evidences the importance of host-guest covalency in the bulk modulus enhancement whereas the effect of ionicity is to decrease it. This is the same tendency as the one proposed²³ for ionocovalent tetrahedrally coordinated compounds.

Let us now turn to the pressure stability of silicon clathrate structures. We can first note the important difference in the values of the phase transition pressure: 11.5, ~14, 13, and 17 GPa for Si-34, Na₈@Si-46, Ba₈@Si-46, and I₈@Si-46, respectively. To understand the origin of such a spread of values, we plot the average Si-Si distance over all the tetrahedral units of the clathrate structure with respect to pressure [Fig. 3(b)]. The empty clathrate values are from Ref. 7 and the Si-2 ones from Ref. 24. We find that the phase transition of all clathrates takes place when the Si-Si average distance attains a value of 2.30 Å [hatched region in Fig. 3(b)]. This suggests that the average host interatomic distance is a determinant parameter for the stability of silicon tetrahedral networks. As shown in Fig. 2(b), in the case of silicon with diamond structure, the interatomic Si-Si distance

can be further reduced before the occurrence of any phase transformation, but the 2.30 Å value is recovered if subjected to strong uniaxial stress.²⁵ In spite of the cubic character of the clathrate structure, the presence of pentagonal and planar hexagonal rings introduces a distribution of distances and angles around those of the regular tetrahedron²⁶ which gives rise to a strongly stressed sp^3 tetrahedra-based structure. This indicates that the same physical process can be at the origin of the stability of silicon clathrates and of diamond silicon.²⁷

Once the critical distance of 2.30 Å is attained, the subsequent pressure evolution strongly depends on the intercalation element. Na₈@Si-46, as Si-34, transforms into the silicon stable phase at the pressure corresponding to the critical distance. The case of the iodine clathrate is very different. The volume variation observed at 17 GPa is within the error bars of the experiment. However, if we attempt to fit all experimental points up to 35 GPa with a single Murnaghan equation of state, we observe that all points lie over the curve before 17 GPa and below it at higher pressures. Even if changes in the fractionary coordinates of atoms may have taken place in the cell, the small volume reduction at 17 GPa is not compatible with a collapse of the cage structure. Consequently iodine clathrate pushes the limit of cage-structure stability up to pressures at least 3 times higher than the stability limit of the empty silicon clathrate. For Ba clathrates, we observe a strong but progressive modification in the slope of the volume reduction with pressure from 13 GPa to 18 GPa, but the cubic structure is preserved at least up to 30 GPa. From that pressure, the weaker diffraction peaks disappear and the ones remaining become weak and enlarge. Nevertheless, no new peaks are observed. Partial amorphization, decomposition, progressive emptying of the silicon cages, or a change on the barium electronic structure²⁸ can be called on for an explanation, but more investigation will be needed to clarify this point.

In the case of Ba₈@Si-46 at the highest pressures, the calculated distance goes below the minimum Si-Si distance of the Si diamond phase (2.28 Å at 11.5 GPa), leading to distances comparable to the ones observed in the high-pressure AlB₂-like phase of CaSi₂.²⁹ In this high-pressure phase of CaSi₂, Si is threefold coordinated with Si bonds forming an angle close to 120° and its electronic hybridization can be considered as sp^2 .²⁹ Consequently, in Ba₈@Si-46, our assumption leads to a Si tetrahedral interatomic distance comparable to the one found in a sp^2 configuration. This observation together with the important modifications in terms of volume and compressibility tends to favor an evolution of the internal coordinates after the phase transition for the Ba clathrate. If this is the case, then the estimate of the average Si-Si distance in Fig. 3(b) for Ba₈@Si-46 after 13 GPa must be taken with caution.

In conclusion, we have shown that intercalation of silicon clathrates can lower the compressibility up to the one of diamond silicon and extent the stability of cage-based structures up to very high pressures. We have further shown that the stability of silicon networks is associated with a limiting silicon interatomic distance. Even though the present results

have been obtained for silicon systems, we believe that the same mechanisms should apply to other cage-based systems and in particular to carbon systems for which important technological applications rely on their compressibility and stability under pressure. Such carbon systems include for example hypothetical carbon clathrates,^{5,7,30} but also polymerized C₆₀ (Refs. 31 and 32), and C₃₆ (Ref. 33) networks, or even bundles of nanotubes. We believe that the

present results open a new line of work for attempting the synthesis of ultrahard materials.

We thank Professor J. P. Gaspard of the University of Liège for very fruitful discussions. We thank the Japanese Society for the Promotion of Science for its partial financial support. X.B. acknowledges the CEA-Grenoble (France) for the use of its supercomputer.

- ¹C. Cros, M. Pouchard, and P. Hagemmuller, C. R. Acad. Sci. URSS **260**, 4764 (1965); J.S. Kasper, P. Hagemmuller, M. Pouchard, and C. Cros, Science **150**, 1713 (1965).
- ²H. Kawaji, H.-o. Horie, S. Yamanaka, and M. Ishikawa, Phys. Rev. Lett. **74**, 1427 (1995).
- ³J.S. Tse *et al.*, Phys. Rev. Lett. **85**, 114 (2000).
- ⁴T. Kawaguchi, K. Tanigaki, and M. Yakusawa, Phys. Rev. Lett. **85**, 3189 (2000).
- ⁵J. Gryko *et al.*, Phys. Rev. B **62**, R7707 (2000).
- ⁶G. B. Adams *et al.* Phys. Rev. B **49**, 8048 (1994).
- ⁷A. San Miguel *et al.*, Phys. Rev. Lett. **83**, 5290 (1999).
- ⁸In our Si-*n* notation, *n* denotes the number of atoms in the primitive unit cell (the diamond structure is then labeled Si-2 and Si-34 and Si-46 replace, respectively, Si₁₃₆ and Si₄₆, which are sometimes found in the literature).
- ⁹M. D. Rutter *et al.*, J. Phys. Chem. Solids **62**, 599 (2001).
- ¹⁰N. F. Mott, J. Solid State Chem. **6**, 348 (1973).
- ¹¹S. Saito and A. Oshiyama, Phys. Rev. B **51**, 2628 (1995).
- ¹²D. Londono, W. F. Kuhs and J. L. Finey, Nature (London) **332**, 141 (1988).
- ¹³W. L. Vos, L. W. Finger, R. J. Hemley and H.-k. Mao, Phys. Rev. Lett. **71**, 3150 (1993).
- ¹⁴J. S. Loveday *et al.*, Nature (London) **410**, 661 (2001).
- ¹⁵J. S. Tse *et al.*, Nature (London) **369**, 724 (1994).
- ¹⁶E. Reny, P. Gravereau, C. Cros, and M. Pouchard, J. Mater. Chem. **8**, 2839 (1998).
- ¹⁷S. Yamanaka, E. Eniswhi, H. Fukuoka, and M. Yasukawa, Inorg. Chem. **39**, 56 (2000).
- ¹⁸E. Reny, S. Yamanaka, C. Cros, and M. Pouchard, Chem. Commun. (Cambridge) **2000**, 2505 (2000).
- ¹⁹These energy minimizations, associated with the spread of the Si-Si first-neighbor distances, yield values of $x=0.183$, $y=0.310$, and $z=0.116$ for the atomic coordinates. These numbers are very close to the ones encountered in Rietveld refinement of clathrates made of very different atoms [S. Bobev and S.C. Sevov, J. Solid State Chem. **92**, 153 (2000)].
- ²⁰P. Hohenberg and W. Kohn, Phys. Rev. **136**, B864 (1964); W. Kohn and L.J. Sham, Phys. Rev. **140**, A1133 (1965).
- ²¹N. Troullier and J. L. Martins, Phys. Rev. B **43**, 1993 (1991); K. Kleinman and D. M. Bylander, Phys. Rev. B **48**, 1425 (1982); A 16 Ry cutoff was used in the plane-wave expansion of the wave function. We have verified that the finite-size basis correction of Rignanese *et al.* [G.-M. Rignanese *et al.*, Phys. Rev. B **52**, 8160 (1995)] did not yield any change in B_0 within 0.3%. Together with the variation of the bulk modulus with the choice of the theoretical data points, the uncertainty for B_0 is estimated to be ± 1 GPa.
- ²²D. Connétable, V. Timoshevskii, E. Artacho, and X. Blase, Phys. Rev. Lett. **87**, 206 405 (2001).
- ²³M. L. Cohen, Phys. Rev. B **32**, 7988 (1985).
- ²⁴*Crystal and Solid State Physics*, edited by K. H. Hellwege and A. Hellwege, Landolt-Börnstein, Numerical Data and Functional Relationships in Science and Technology, New Series, Group III, Vol. I (Springer-Verlag, Berlin, 1966).
- ²⁵J. Z. Hu, L. D. Merkle, C. S. Menoni, and I. L. Spain, Phys. Rev. B **34**, 4679 (1986).
- ²⁶P. Mélinon *et al.*, Phys. Rev. B **59**, 10 099 (1999).
- ²⁷We can recall here that silicon is at the edge of the “polarizability catastrophe” [P. Edwards and M. J. Sienko, Chem. Br. **19**, 39 (1983)] and that the most direct way of going through that edge is the application of pressure. This will drive a semiconductor to metal transition, which in our case will correspond to a charge delocalisation of the Si-host sp^3 network. The observed phase transitions could then be interpreted as driven via such electronic instability of the sp^3 network.
- ²⁸M. Ross and A. K. McMahan, Phys. Rev. B **26**, 4088 (1982).
- ²⁹P. Bordet *et al.*, Phys. Rev. B **62**, 11 392 (2000).
- ³⁰S. Saito and A. Oshiyama in *Recent Advances in the Physics and Chemistry of Fullerenes and Related Materials*, edited by K. M. Kadish and R. S. Ruoff (Electrochemical Society, Pennington, 1996), Vol. 3, p. 457.
- ³¹L. Marques *et al.*, Science **283**, 1720 (1999).
- ³²E. Burgos *et al.*, Phys. Rev. Lett. **85**, 2320 (2000) and references therein.
- ³³C. Piskoti, J. Yarger, and A. Zettl, Nature (London) **393**, 771 (1998); J. C. Grossman, M. Cote, S. G. Louie, and M. L. Cohen, Phys. Rev. Lett. **81**, 697 (1998).